

An Earth-Based Equivalent Low Stretch Apparatus to Assess Material Flammability for Microgravity & Extraterrestrial Fire-Safety Applications

S.L. Olson*,

NASA Glenn Research Center, Cleveland, OH 44135

H. Beeson, and J.P. Haas,

NASA White Sands Test Facility, Las Cruces, NM

Abstract

The objective of this project is to modify the standard oxygen consumption (cone) calorimeter (described in ASTM E 1354 and NASA STD 6001 Test 2) to provide a reproducible bench-scale test environment that simulates the buoyant or ventilation flow that would be generated by or around a burning surface in a spacecraft or extraterrestrial gravity level. This apparatus will allow us to conduct normal gravity experiments that accurately and quantitatively evaluate a material's flammability characteristics in the real-use environment of spacecraft or extra-terrestrial gravitational acceleration. The Equivalent Low Stretch Apparatus (ELSA) uses an inverted cone geometry with the sample burning in a ceiling fire configuration that provides a reproducible bench-scale test environment that simulates the buoyant or ventilation flow that would be generated by a flame in a spacecraft or extraterrestrial gravity level. Prototype unit testing results are presented in this paper. Ignition delay times and regression rates for PMMA are presented over a range of radiant heat flux levels and equivalent stretch rates which demonstrate the ability of ELSA to simulate key features of microgravity and extraterrestrial fire behavior.

Introduction

NASA's current method of material screening determines fire resistance under conditions representing a worst-case for normal gravity flammability - the Upward Flame Propagation Test (Test 1^[1]). The applicability of Test 1 to fires in microgravity and extraterrestrial environments, however, is uncertain because the relationship between this buoyancy-dominated test and actual extraterrestrial fire hazards is not fully understood. Flames in micro-gravity are known to preferentially spread upwind^[2], not downwind as in the normal gravity upward flammability screening Test 1. At low flow velocities, the concurrent (Test 1 configuration) flame spread was not viable over vertical solid cylinders, while the stagnation point flame at the bottom end of the cylinder (low stretch flame) was viable^[3,4]. In addition, the maximum flammability in the upwind spread configuration is known to be at lower imposed flows and lower oxygen concentrations than in normal gravity^[5].

Theoretical predictions by Foutch and T'ien (1987)^[6] indicate that it should be possible to understand a material's burning characteristics in the low stretch environment of spacecraft (non-buoyant, but with some movement induced by fans and crew disturbances) by understanding its burning characteristics in an equivalent Earth-based stretch environment (induced by normal gravity buoyancy). Experimental results^[7] demonstrate the transition from a robust flame at stretch rates of 10-20 s⁻¹ to a quenched flame at very low stretch (1-2 s⁻¹) in air where the stretch rate is purely buoyant. In these tests, sample radius of curvature was the primary variable controlling the stretch rate, but this is not convenient for standardized testing.

Experiment Setup

The ELSA apparatus, shown conceptually in Figure 1, uses a mass-flow controlled forced-air flow issuing from a 7.5 cm diameter nozzle into the cone to augment the low buoyant stretch. Stretch rates have been varied in a prototype facility from purely buoyant (estimated ~ 3.5 s⁻¹ for the 28 cm sample plate) to 33.5 s⁻¹ with forced convection. Cone heat flux has been varied from 10-25 kW/m². Samples are mounted 2.5 cm above the cone, which is the same distance as the normal cone configuration.

The samples used are 2.4 cm thick PMMA, cut to the standard cone test sample size of 10 cm x 10 cm exposed surface area, but also have

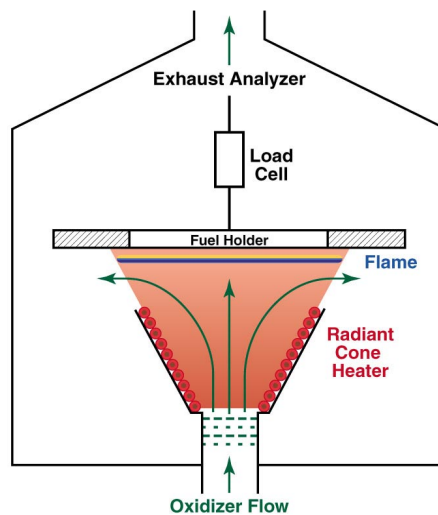


Figure 1: Concept of ELSA apparatus, showing fuel sample suspended above radiant cone heater and oxidizer flow jet. The enclosure reflects the WSTF Controlled Atmosphere Cone Calorimeter facility^[1].

* Dr. Sandra L. Olson, Sandra.olson@grc.nasa.gov

a 2.5 cm lip around the opening to prevent the sample from falling through the opening. The holder is 0.2 cm thick stainless steel, 28cm wide.

The test procedure first establishes the cone heat flux using a heat flux gauge. The low velocity flow is established and then the sample moved into position to expose it to this environment. It should be noted that the net heat flux increases due to the addition of convective flow. The pilot (hot source or spark) was positioned to the side of the sample, very near the surface of the plate to ignite the vapors once a flammable mixture is obtained. Thermocouples on the surface of the sample record the surface temperature, video cameras record the ignition and flame behavior. The air mass flow rate, radiant flux and cone temperature are recorded as well.

Once burning is established, the flame reaches a “pseudo-steady state” in approximately 10 seconds. Because the sample is of intermediate thickness, the interior continues to heat up throughout the test time, so true steady state is never obtained.

Equivalent stretch rates can be determined as a function of gravity, imposed flow, and geometry. For purely buoyant flow, the equivalent stretch rate is $a_b = [(\rho_c - \rho^*)/\rho_c] [g/R]^{1/2}$ ^[6,7], where the density difference from the average flame temperature to ambient is used, g is gravity, and R is the radius of curvature of the sample. For purely forced flow, the equivalent stretch rate is characterized by either $a_f = 2U_\infty/R$ for a cylinder^[6], or $a_f = U_{jet}/d_{jet}$ for a jet impinging on a planar surface^[8]. U is the velocity of the ambient stream or the jet, R is the radius of curvature of the cylinder, and d is the diameter of the jet. A generalized expression for stretch rate which captures mixed convection includes both buoyant and forced stretch is defined^[6] as $a_{equivalent} = a_f(1 + a_b^2/a_f^2)^{1/2}$.

The contributions of the buoyant stretch on the equivalent stretch rate were evaluated by correlating regression rate data for flat disks of various radii^[9] and cylindrical samples with reported stretch rates^[7]. The correlation, shown in Figure 2, allows us to determine the inherent buoyant stretch for ELSA to be $\sim 3.5 \text{ s}^{-1}$ by matching the regression rates for cylinders and flat disks. Note that this correlation worked even through the range of radii where Rayleigh-Taylor instabilities were found at larger radii (>8cm)^[9].

Results and Discussion

Ignition

The samples are radiantly ignited with the assistance of a gas-phase pilot (a hot source or spark) to ignite the vapors. Ignition of the sample was recorded on video, and the time to ignition determined for each test condition.

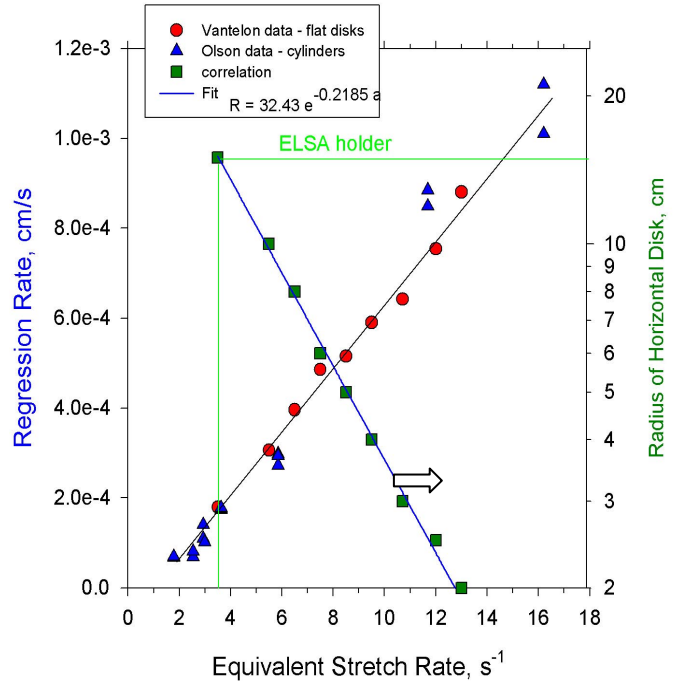


Figure 2: Linear correlation of flat disk radius with equivalent buoyant stretch^[7,9]. Regression rates for cylinders and flat disks were correlated, and the equivalent stretch rate for the 14 cm radius ELSA holder determined from the linear relation found between radius of the disk and equivalent stretch rate.

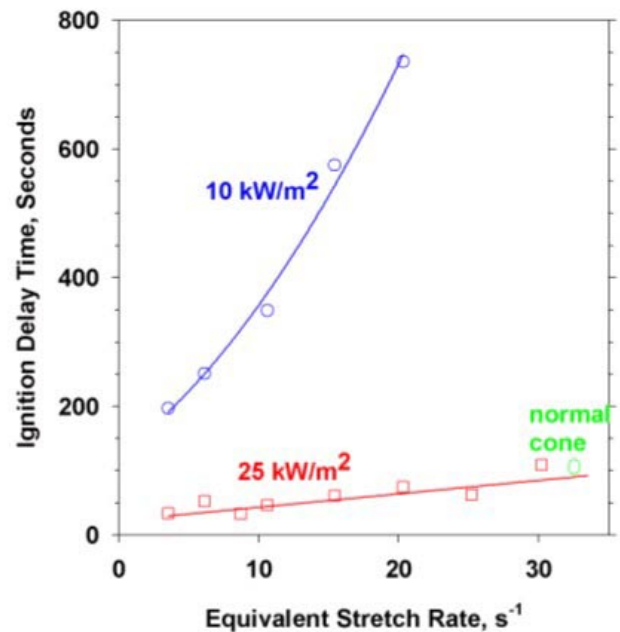


Figure 3 Ignition delay times as a function of equivalent stretch rate.

Ignition delay times were measured at 10 kW/m^2 and 25 kW/m^2 flux levels, as shown in Figure 3. For a fixed radiant flux, ignition delay times are shown to decrease with decreasing stretch rate. The difference between a normal cone ignition delay time and ignition delay times at very low stretch is a factor of three, demonstrating that ignition delay times determined from normal cone tests significantly *overestimate* the ignition delay times of materials in microgravity or in low stretch extraterrestrial environments. In addition, at the 10 kW/m^2 flux level, the ignition delay time at low stretch approaches the value of the normal cone at 25 kW/m^2 , indicating the sensitivity of low stretch flames to even weak levels of external flux.

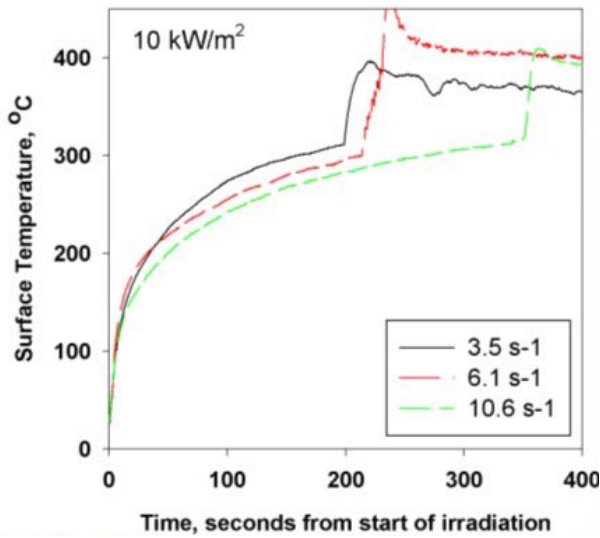


Figure 4: Surface temperature histories as a function of stretch rate for 10 kW/m^2 cone heat flux.

Cellular Instabilities

Due to the flat sample geometry, at low forced stretch rates, Rayleigh-Taylor instabilities were observed beneath the sample. These instabilities were not observed for curved samples^[7]. The instabilities in these tests were notably worse at higher flux levels, where fuel vaporization rates are quite vigorous.

Figure 5 shows the decrease in the cellular instabilities with increasing stretch. The nominal transition from cellular planar occurs at $\sim 8 \text{ s}^{-1}$.

While the cellular instability is clearly gravity dependent, its development occurs well after ignition. Thus ignition delay time and ignition temperature data is not affected by this instability. The pseudo-steady-state flame shape is dominated by this instability. It is less clear whether average burning rates are significantly affected, as will be discussed below.

Surface Regression

After ignition, samples were allowed to burn for a period of time in order to obtain information about the average burning rates of the material. For all stretch rates, the samples were found to regress uniformly across the exposed area, which indicates that the Rayleigh-Taylor cells do not affect the fuel surface regression locally. It is less clear if the cellular flow field significantly affects the burning rate in a global sense. Due to the enhanced convection, the burning rates could be higher than they would be without the cellular flow. On the other hand,

Surface temperature was also recorded during tests. Figure 4 shows surface temperature rising as a power law relation once the sample is exposed to the cone heat flux, as would be expected for a slab with constant heat flux at the surface. Ignition is noted by a sudden jump in temperature in each test. The ignition temperature is defined as the temperature at which this jump starts. The surface temperatures at ignition decreased with increasing stretch, and were lower at lower imposed flux levels, and the slope is similar for both flux levels, reflecting the effect of the additional convective heat transfer on ignition.

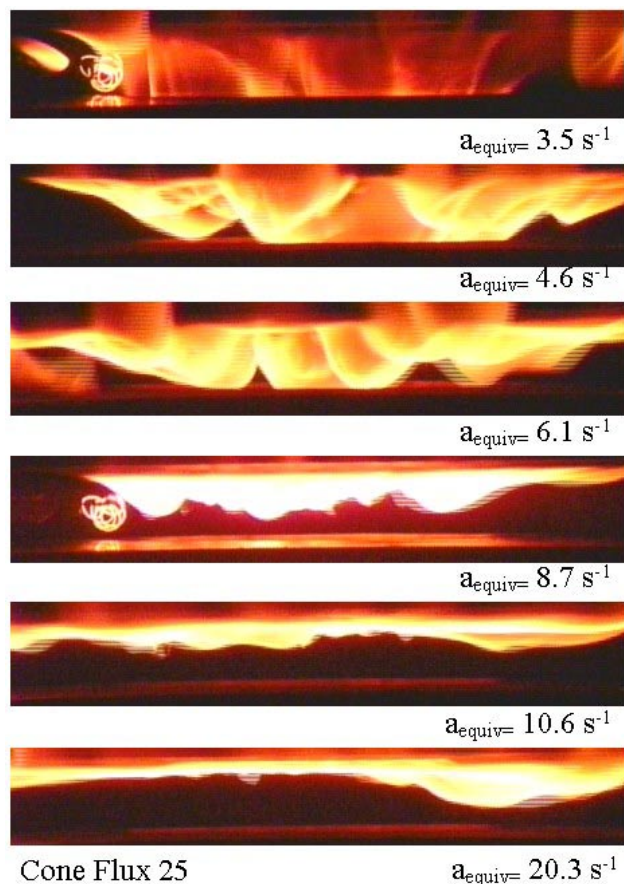


Figure 5: Rayleigh-Taylor instabilities are observed at stretch rates less than $\sim 8 \text{ s}^{-1}$. These instabilities are due to the flat samples used in these experiments as well as the augmented heat flux levels. At low stretch rates, the cells are very large, and extend into the cone.

they could be lower because of the larger average standoff distance between the flame and the fuel surface.

Average regression rates, shown in Figure 6, were obtained by weighing the samples before and after the test and dividing the mass loss by the test time, exposed area and density ($\rho = 1.19 \text{ g/cc}$, $A = 100 \text{ cm}^2$). Regression rates increase with heat flux and stretch rate, but regression rates are much more sensitive to heat flux at the low stretch rates. A modest increase in heat flux of 25 kW/m^2 increases the burning rates *by an order of magnitude* at the lower stretch rates. These trends are reasonable for low stretch flames, which have been shown to be very sensitive to the ratio of heat loss to heat generated via combustion^[7].

Even at 10 kW/m^2 , the cone heater offsets the surface radiative loss, which is significant relative to the weak heat generation rates^[7]. Thus, low stretch flames with these losses offset may find themselves vaporizing much more fuel than there is oxygen available with which to react. The products of combustion from such flames will be more toxic (CO, soot, THC, etc.) in addition to posing a significant risk of buildup to explosive levels in a confined space.

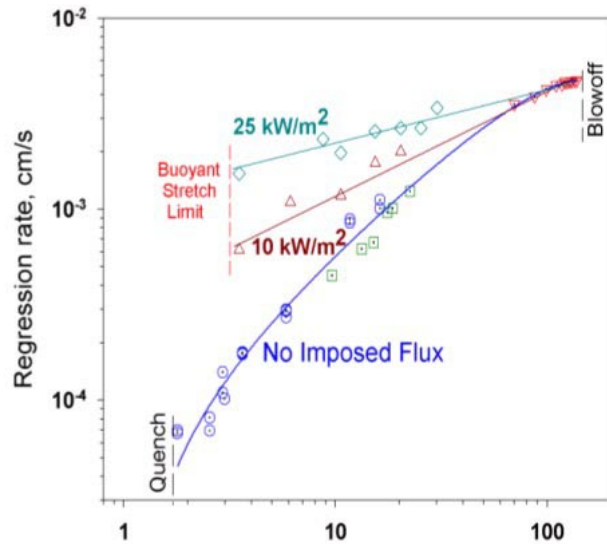


Figure 6 : PMMA regression rates for three levels of imposed heat flux from radiant cone heater, plotted as a function of equivalent stretch rate. Data: \diamond , Δ this work, \circ ^[7], \square ^[10], ∇ ^[8].

Conclusions

The Equivalent Low Stretch Apparatus (ELSA) uses an inverted cone geometry with the sample burning in a ceiling fire configuration that allows for low stretch stagnation flow. Ignition delay times and regression rate data have been measured in a prototype unit.

For a fixed radiant flux, ignition delay times for PMMA are shown to decrease by a factor of three at low stretch, demonstrating that ignition delay times determined from normal cone tests significantly underestimate the risk in microgravity.

Regression rates for PMMA increase with heat flux and stretch rate, but regression rates are much more sensitive to heat flux at the low stretch rates, where a modest increase in heat flux of 25 kW/m^2 increases the burning rates by an order of magnitude.

These results demonstrate the ability of ELSA to simulate key features of low stretch materials flammability behavior. ELSA provides a new tool to assess microgravity and extraterrestrial fire hazards.

Acknowledgements

The authors would like to acknowledge NASA Glenn engineers Chris Gallo for designing the prototype unit and Ray Wade for designing the spark ignition system.; summer students Lander Coronado-Garcia and FloJaune Griffin for conducting many of the prototype experiments; and Jayme Baas and Sarah Smith for their work on the engineering modifications to the WSTF ELSA apparatus.

References

- 1) NASA-STD-6001, 1998.
- 2) McGrattan, K.B., Kashiwagi, T., Baum, H.R., and Olson, S.L.; *Combustion and Flame (C&F)*, V. 106, pp.377-391, 1996.
- 3) Halli, Y., and T'ien, J.S., NBS-GCR-86-507, Feb. 1986.
- 4) Ivanov, A.V, et. al, NASA Contract NAS3-97160 final report, Russian Space Agency, Keldysh Research Center, Moscow 1999, also NASA CP-1999-208917, pp. 47-50.
- 5) Olson, S.L., *Comb. Sci. & Tech.* V. 76, pp.233-249, 1991.
- 6) Foutch, D.W., & T'ien, J.S., *AIAA J.*, V.25, No.7, pp.972-6, 1987.
- 7) Olson, S.L and T'ien, J.S.; *C.&F.*, V.121, pp.439-452, 2000.
- 8) T'ien, J.S., Singhal, S.N., Harrold, D.P., and Prah, J.M.; *Combustion and Flame*, Vol. 33, pp.55-68, 1978.
- 9) Vantelon, J.P., Himdi, A., and Gaboraiud, F.; *Combust. Sci. and Tech.*, V54, pp. 145-158, 1987.
- 10) Ohtani, H., Akita, K., and Hirano, T., *Combustion and Flame*, Vol. 53, pp. 33-40, 1983.